

Autonomous peak-picking procedure for tension force estimation in cables and external post-tensioning tendons

Luis Chillitupa-Palomino¹, 0009-0001-5274-0436, Carlos M.C. Renedo¹, 0000-0003-1014-0878, Jaime H. Garcia-Palacios², 0000-0003-4336-5520, Iván M. Díaz¹, 0000-0001-9283-5109

¹Department of Continuum Mechanics and Theory of Structures, ETSI Caminos, Canales y Puertos, Universidad Politécnica de Madrid, Calle Profesor Aranguren 3, Madrid, 28040, Comunidad de Madrid, Spain

²Department of Hydraulics, Energy and Environmental Engineering, ETSI Caminos, Canales y Puertos, Universidad Politécnica de Madrid, Calle Profesor Aranguren 3, 28040 Madrid, Spain

email: luis.cpalomino@upm.es, carlos.martindelaconcha@upm.es, jaime.garcia.palacios@upm.es, ivan.munoz@upm.es

ABSTRACT: Cables and external post-tensioning tendons are key elements of modern strategic bridges; however, their structural integrity has been questioned due to some structural collapses registered during the last decades. In this context, cost-effective vibration-based monitoring strategies can be implemented to improve their maintenance by continuously estimating their tension force (a key damage indicator) from their natural frequencies. These frequencies may vary in time due to environmental changes, modification of the service loads, and tensioning processes produced during cable substitution manoeuvres. In monitoring systems that only use one accelerometer per cable (the most common situation in practice), a robust and accurate peak-picking method is required to adequately identify which are their actual almost harmonic natural frequencies and to which modal order they correspond to. Ideally, this method should be automated (to run continuously), autonomous (with as few hyperparameters as possible) and self-regulating (to discard poor quality spectra and outliers). Additionally, the method must be able to cope with two well-known phenomena experienced in practice that dirt cable spectra: i) the double peak effect, and ii) the presence of bracing belts between cables. Thus, this paper works on developing an autonomous peak-picking procedure to cope with the aforementioned phenomena for enabling a reliable tension force estimation method in cable structures. This methodology has been applied to a one-week monitoring data set of measurements of real external post-tensioning tendons of a road bridge in Spain.

KEY WORDS: Cable dynamics, Tension estimation, Post-tensioning tendons, Automatic peak-picking, Condition monitoring

1 INTRODUCTION

Cables and tendons are crucial elements in bridge engineering but also are vulnerable structural elements because they are usually subjected to fatigue and corrosion problems. Thus, vibration-based non-destructive techniques have been used for external post-tensioning tendon assessment. The main parameter to assess in these cases is the tension force, as this performance indicator can give a clear idea of the condition of the cable and thus, the overall condition of the structure. The tension force is usually estimated from the measured natural frequencies, which are used to inversely solve the dynamic equation of an elastic tensioned cable.

The higher the number of natural frequencies identified, the better the tensile force estimation. Indeed, the estimation of several natural frequencies results compulsory when the bending stiffness of the cable is not negligible. However, this frequency identification is especially challenging when only one accelerometer is employed for monitoring the element, as in these cases, it has to be performed by detecting peaks on the vibration signal's power spectral density (PSD). In the case of simply-supported cables, when their bending stiffness is negligible, the frequencies of these peaks should be perfectly periodical (which corresponds to the blue straight line in Figure 1, where the frequency values are represented against their modal orders). When the bending stiffness has a considerable influence on the cable dynamics, these frequencies are quasi-periodical, gradually increasing the distance between

consecutive peaks. This effect can be clearly seen in the orange line of Figure 1.

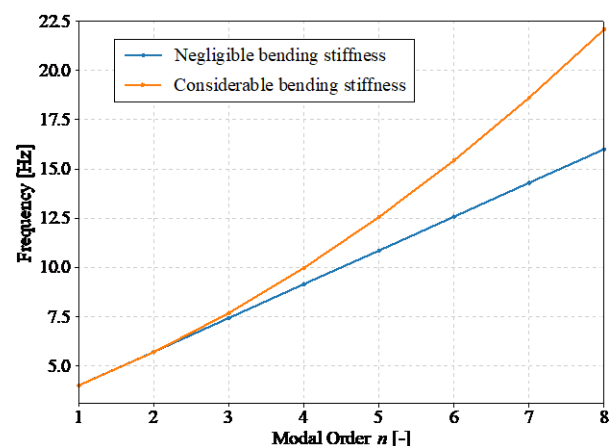


Figure 1: Effect of bending stiffness on natural frequencies.

Although peak-picking may appear to be simple, some issues make difficult the identification procedure and its automatization. First, the variation over time of the natural frequencies to be identified makes more suitable methods that do not use initial guessing values to detect these peaks. Second, the presence of double peaks (doublets) within the PSD. This is caused due to the fact that the cable section may not be perfectly symmetric and thus, certain bending modes may decompose in couples of closely-spaced peaks. Third, the presence of bracing

belts between homologous cables may couple their similar but not identical vibration, also contributing to create doubles. Fourth, in external post-tensioning tendons running through several spans, the vibration of the different sections of the cable between deviators (with different span lengths) may be coupled, providing dirty spectra in which harmonics of neighbouring cable segments are mixed. Finally, interactions between the measured cable and other structural elements may dirt the PSD signals, thus, perturbing the frequency identification process and provoking an unreliable tension estimation. A typical situation of this type occurs in cable stayed bridges, when the vibration of the deck is transmitted to the stay cables or hangers.

Some authors have faced in the past the problem of developing a real-time and automatic frequency identification methodology for performing an accurate tension estimation in cable elements. This automatization has been solved in a variety of ways within the literature. Most of them detect these frequencies by performing an automatic peak-picking process from the signal's PSD. Initially, Cho et al. [5] belowproposed a simple iterative process that lacked the necessary robustness. Then, Sim et al. [6] studied a frequency tracking method based on providing reference initial guessing values around which the peak search is performed. They claim its validity based on two facts: i) the frequencies variation due to environmental changes are small, and ii) the searched peaks are well-separated.

Regarding deep learning applications, Kim et al. [7] have developed a tool based on object detection for performing automatic peak-picking from PSDs images with a region based convolutional neural network (a similar method is researched by Chen et al. [9]). The main advantage of this approach lays on the fact that no guessing values need to be provided, although the robustness of these tools rely on their training data set. Later, Jeong et al. [8] applied this latter method for performing automatic tension estimation on cables. They worry about the detection of undesired peaks not corresponding to cable natural frequencies. For that, they use the frequency distance between peaks, also named as 'interval'. The main drawbacks of such a methodology will be discussed later. However, they do not cover issues as: i) how to correctly assign the modal order to each peak, ii) how to manage missing peaks that interrupt a series of consecutive frequencies, and iii) how optimize the computational cost for its proper in-line implementation in continuous monitoring systems.

One of the most revealing contributions is the one by Zhang et al. [10] that provided a clear explanation of the main challenges arising when performing tension estimation from cable vibration data, namely: i) detection of useful PSDs with recognizable peaks, ii) automatic and robust identification of frequency peaks, and iii) assignation of modal orders to the identified frequencies. They proposed a simple methodology based on updating a threshold prominence value till a minimum number of peaks has been identified. After this, they discard fake peaks if their frequency is not a multiple of the most common value for the interval. With this same principle, they assign the modal order to the peaks. This method results quite applicable to cables with low-bending stiffness (EI), however, when EI is remarkable, its applicability is limited, as proportionality is lost for higher modes. Another important contribution is the one of Jin et al. [2] in which the automated

peak-picking is covered in detailed, remarking important facts such as the necessity of removing the baseline from the PSD curve to assess all the peaks with the same floor level. Their proposal is based on the application of a breakthrough multiscale-based peak detection algorithm (previously developed by [1]) combined with a criterion based on the median absolute deviation of the detected peaks. They compared this method with the one developed by Jeong et al. [8] confirming a substantial enhancement. Despite this, they do not provide any strategy to detect false peaks apart from the robustness of the method.

The present research provides a modified methodology for performing autonomous peak-picking detection based on the findings by Jin et al. [2]. To the authors knowledge, all the contributions covering autonomous tension estimation of cable structures have dealt with long cables of cable-stayed bridges with EI not influencing their dynamic. This paper, for the first time, addresses this automatization problem in much shorter external post-tensioning tendons with non-negligible EI influence.

This paper has been structured as follows: after the present section, Section 2 presents the autonomous peak-picking methodology. Section 3 illustrates a variation of the methodology for its in-line integration into a continuous monitoring system. Section 4 demonstrates the application of the methodology to data obtained from a week-long continuous monitoring measurement in an in-service post-tensioning tendon. Finally, Section 5 provides some conclusions and future works.

2 AUTONOMOUS PEAK PICKING METHODOLOGY

As mentioned before, an autonomous peak-picking method is an essential previous element to continuously estimate the tension force of cables from a single vibration measurement registered within a continuous monitoring application. The present paper proposes a method for that, based on the contribution of Jin et al. [2] in which the main innovation is the implementation of the so-called multi-scale peak detection algorithm previously developed by [1]. This algorithm, which is the core of the method, was conceived to detect periodic peaks within signals (indeed, it has been applied to detect heart beats). This is done through building the so-called local maximum scalogram (LMS) of the signal being analysed. A scalogram is a graphical representation of a given signal's magnitude, resulting from analysing it using moving windows of different scale (number of samples). With the LMS, it can be detected the particular scale related to the interval of the periodic peaks being searched. Jin et al. [2] applied this concept to successfully analyse the PSDs of cable vibrations.

On the one hand, for smoothly detecting environmental changes on the natural frequencies of cables, a great frequency resolution, $\Delta f = 1/T$ (T being the duration of the time-domain measured signal) and high sampling frequencies are required to detect a significant number of harmonics, are needed within the PSDs to be analysed. On the other hand, if these PSDs are such long vectors, the computational cost and memory involved on computing their LMS matrices may prevent from performing this process in real time within a continuous monitoring loop (the complexity of the problem is $O(n^2/2)$). To cope with this issue, a two-step procedure has been proposed: i) developing

the LMS of a low-resolution PSD for roughly detecting the frequencies of the harmonic peaks. Then, frequency bands for later searching them more precisely are created, and ii) searching the final frequency values within a high-resolution PSD using these bands. Apart from these aspects, the following sections cover other considerations which are capital for successfully implementing the methodology in practice when dealing with post-tensioning tendons.

2.1 Signal pre-processing

This process has been depicted in Figure 2. First, the time signal obtained from the monitoring system is detrended to eliminate any drifting caused by many factors, such as instrumental nonlinearity or signal offsets. Then, a low-pass filter is applied to eliminate peaks belonging to unimportant high frequency vibration that might shadow the actual peaks of interest. Furthermore, the filter cutoff frequency should be in accordance with the higher frequency order of interest for the posterior tension force estimation. Finally, the data is resampled (first interpolated and then decimated) to convert the original low-filtered signal to a lower rate in accordance with the low cutoff frequency.

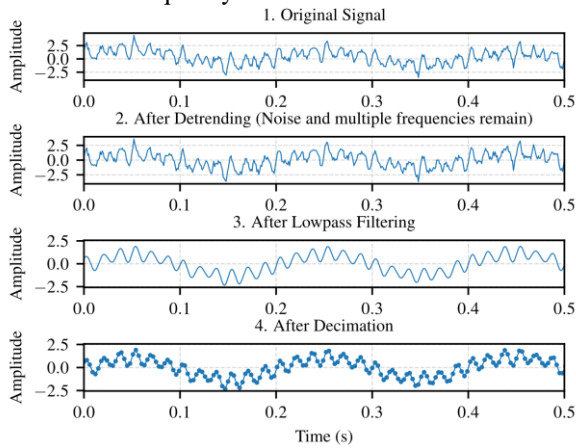


Figure 2: Signal pre-processing steps.

2.2 Low-resolution PSD of the signal

As previously mentioned, a low-frequency-resolution PSD is employed as a workaround to mitigate the high computational cost associated with generating a LMS from a PSD with sufficient frequency-resolution to capture the variation of natural frequencies with temperature. This first PSD is obtained applying the Welch's method using a high averaging of short time windows.

2.3 Baseline correction

Baseline correction is a crucial step in the methodology, as the shape of the spectrum can affect the algorithm's ability to detect certain peaks. Figure 3 provides an example of this process for a cable PSD. To ensure optimal performance, various methods such as polynomial-based, morphological, and asymmetric least squares have been investigated within the literature.

For the baseline correction there are many alternatives such as using the Savitsky-Golay filters, as mentioned in [2], but as indicated in [3], a better alternative is to rely on the use of asymmetric least squares smoothing.

The idea is that for a signal vector \bar{y} with a number of samples equal to m , there should be a 'baseline' signal \bar{z} of equal length that meets the two following characteristics: i) being enough faithful to \bar{y} , and ii) being smooth. Hence, the following least squares function, S , can be built to add together these two effects:

$$S = \sum_i^m \omega_i (y_i - z_i)^2 + \lambda \sum_i^m (\mathcal{A}^2 z_i)^2, \quad (1)$$

where i is an index corresponding to each sample of the signal, and ω_i and λ are a penalty parameter, and a smoothing parameter, respectively, both controlling the balance between these two characteristics. The first term of this equation measures the baseline 'fidelity' to the original signal, while the second one regulates the 'roughness' of the baseline.

The higher the value of S , the less these two requirements are fulfilled. Thus, S must be minimized in terms of \bar{z} , to find an optimal baseline ($dS/d\bar{z} = 0$). After that, the following matrix expression can be derived, from which the vector \bar{z} can be obtained:

$$(\mathbf{W} + \lambda \mathbf{D}' \mathbf{D}) \bar{z} = \mathbf{W} \bar{y}, \quad (2)$$

where \mathbf{D} is a backward second-order-finite-difference matrix and \mathbf{D}' its transpose. \mathbf{W} is a weighted penalty diagonal matrix composed of ω_i values obtained as follows:

$$\omega_i = \begin{cases} p & , y_i > z_i \\ 1 - p & , y_i < z_i \end{cases}, \quad (3)$$

where p is a small value between $[0.1, 0.001]$ which represents an asymmetry factor to consider the fact that a PSD baseline is usually underneath the original PSD. This factor determines a low penalty for positive residuals ($y_i > z_i$) compared to a high penalty applied to negative residuals ($y_i < z_i$).

The baseline correction is an iterative process that starts assigning initial values to ω_i . After that, \bar{z} and ω_i are iteratively computed using (2) and (3) till achieving convergence. Among all, λ is the most influential factor in this process. Its value must be manually set between $[10^2, 10^9]$.

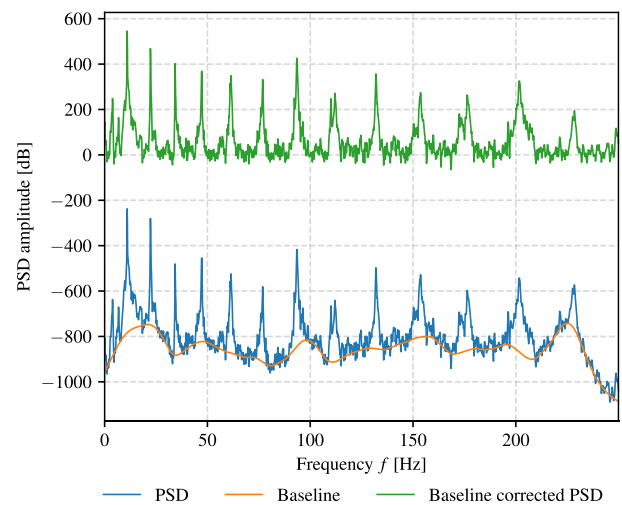


Figure 3: Baseline and baseline corrected PSD.

2.4 Local maxima scalogram and optimal scale selection

From the low-resolution baseline-corrected PSD a LMS is created. This is done by analysing the PSD with a series of moving windows with different number of samples w_k , defined as two times the ‘scale’ of the window k ($w_k = 2k$). This scale is a natural number ranging from 1 to L , being defined as $L = \text{ceil}(N/2) - 1$, being N the total length of the PSD.

Every window of scale k runs through the signal sample by sample. Considering j as the sample index on which the window is centrally positioned, for a given scale k , j will vary from $[k + 1, N - k]$. The LMS is a matrix of dimensions $L \times N$ composed of $m_{k,j}$ elements resulting from moving different windows along the PSD samples. Each $m_{k,j}$ is obtained using a subset of three samples contained within a given window, namely, the two window edges and the central sample $[y_{j-k}, y_j, y_{j+k}]$ (see Figure 4). Thus, $m_{k,j}$ is computed as follows:

$$m_{k,j} = \begin{cases} 0, & \text{if } y_j = \max(y_{j-k}, y_j, y_{j+k}) \\ r + 1, & \text{otherwise} \end{cases} \quad (4)$$

where r is a random number between 0 and 1. Finally, the LMS matrix, \mathbf{M} , gets the form:

$$\mathbf{M} = m_{k,j} = \begin{bmatrix} m_{1,1} & \cdots & m_{1,N} \\ \vdots & \ddots & \vdots \\ m_{L,1} & \cdots & m_{L,N} \end{bmatrix} \quad (6)$$

Thus, \mathbf{M} is a matrix whose elements $m_{k,j}$ indicate whether the current PSD j^{th} value is higher than the neighbours at the edges of the corresponding window with scale k . A graphical representation of \mathbf{M} is given in Figure 5 (white colour corresponds to zero values around the peak regions).

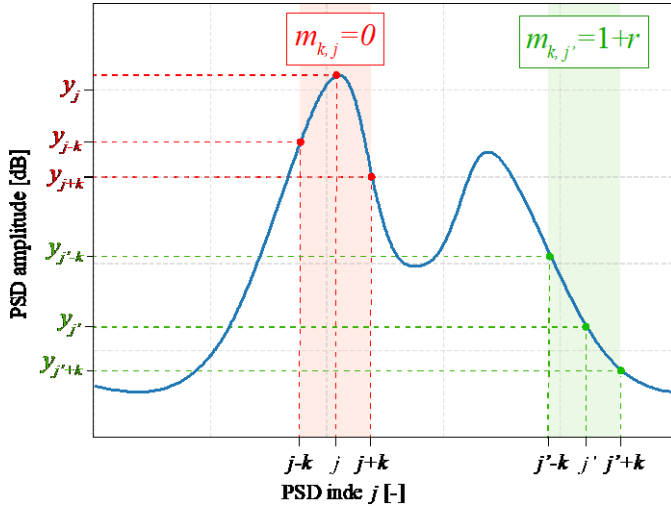


Figure 4: Subset value.

Once the LMS has been created, a row-wise summation is performed in the matrix to obtain the vector $\bar{\gamma}_k$ (represented in Figure 6 as a function of k) as follows:

$$\bar{\gamma}_k = \sum_{j=1}^N m_{k,j}. \quad (6)$$

The scale for which the value of this vector is minimum, k_{min} is the one accounting with more zero values, thus, it corresponds to the rate of appearance of quasiperiodic peaks in the PSD. This value is obtained as follows:

$$k_{min} = \{k \in \mathbb{N} \mid \gamma_{k_{min}} = \min(\bar{\gamma}_k)\} \quad (7)$$

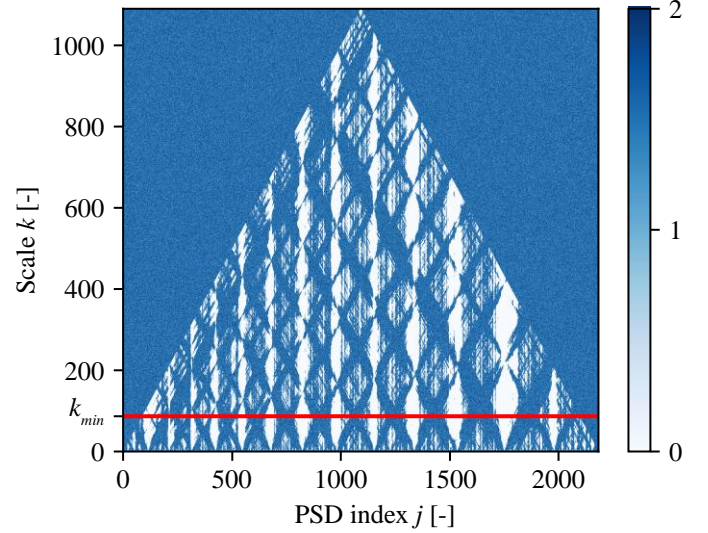


Figure 5: Complete scalogram of baseline-corrected low-resolution PSD.

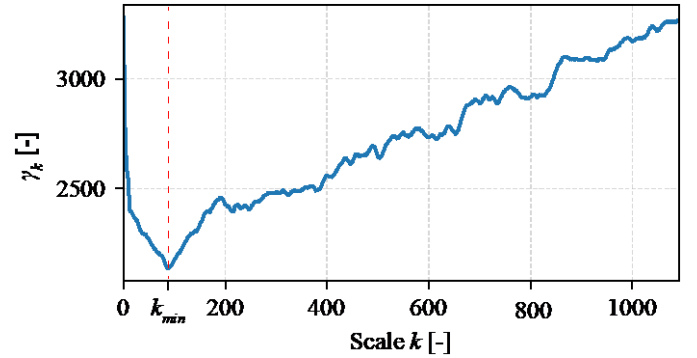


Figure 6: Minimum k scale identification.

Although the methodology works reasonably well, there might detect fake peaks near the PSD borders. To address this issue, it is recommended to add zero-padding to each side of the baseline-corrected-PSD. The extension of this padding must be in proportion with the length of the PSD.

2.5 Rescaled LMS and column-wise sum

After obtaining k_{min} the scalogram is ‘cut’ only considering scales ranging from 1 to k_{min} . In this reduced version of the LMS a column-wise summation is performed to identify PSD samples whose overall sum is zero. This means that for every scale from 1 to k_{min} these particular samples with index $j_{n,low}$ have a zero value in the scalogram, and therefore, they can be identified as peaks corresponding to cable’s natural frequencies $f_{n,low} = j_{n,low} \Delta f$ in the PSD. Figure 7 shows the reduced LMS with red vertical lines indicating the columns where the $j_{n,low}$ values are located.

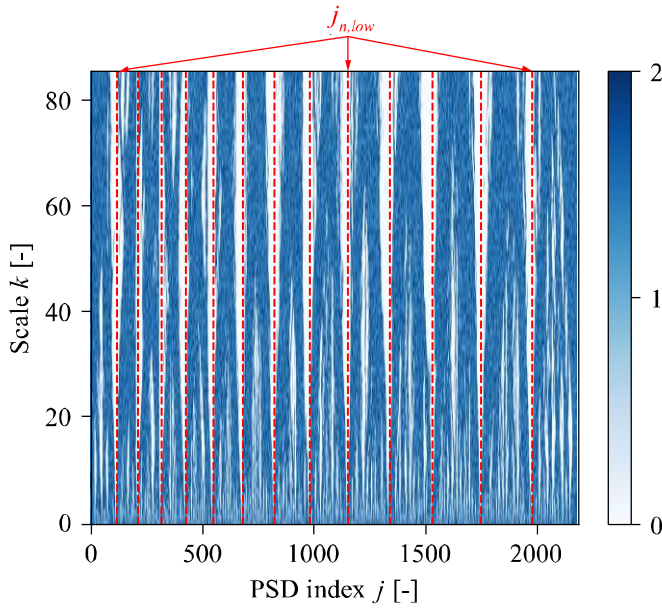


Figure 7: Rescaled LMS.

2.6 High-resolution PSD peaks identification

Once the peak regions have been located within a low-resolution PSD, the final peaks positions need to be precisely identified within a high-resolution PSD. This high-resolution PSD is computed using the Welch's method, considering much longer window lengths (half of the overall signal length) with a 50% of overlapping. Additional zero-padding is applied to each signal segment to improve the frequency resolution.

Within the high-resolution PSD, a precise search is performed in frequency bands associated to each $f_{n,low}$ within the intervals $\left[f_{n,low} - \Delta f \cdot \left(\frac{k_{min}}{4}\right), f_{n,low} + \Delta f \cdot \left(\frac{k_{min}}{4}\right)\right]$. The final natural frequency f_n is the one associated to the maximum of the high-resolution PSD value within the above interval. Figure 8 illustrates the aforementioned high-resolution PSD peak identification procedure.

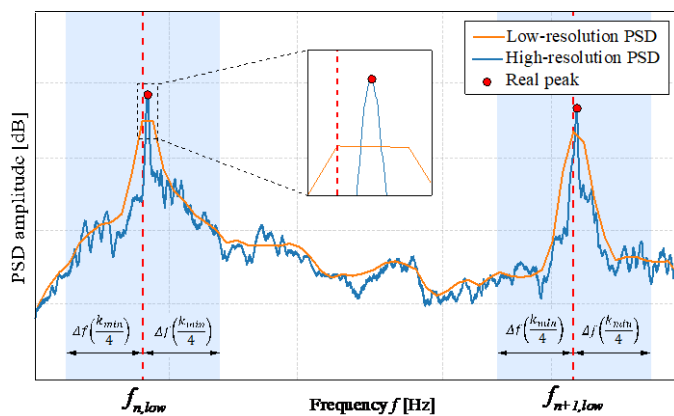


Figure 8: High-resolution PSD peaks identification scheme.

Applying this methodology to a PSD resulting from the vibration measurement of a cable, the results obtained are displayed in Figure 9.

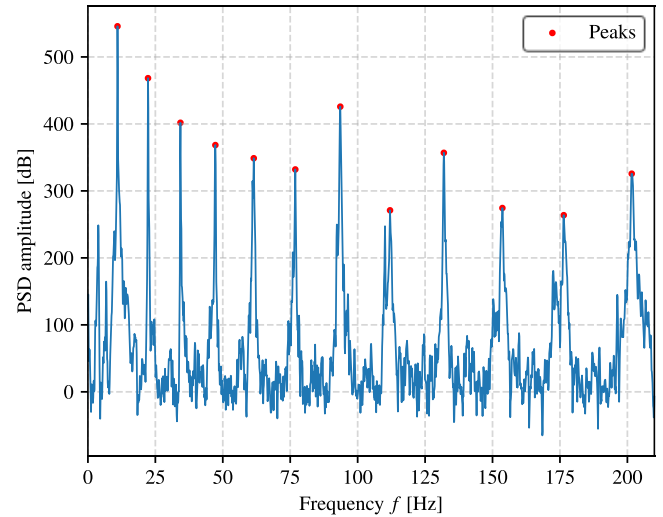


Figure 9: High-resolution PSD with the identified peaks.

3 EXAMPLE OF APPLICATION

The procedure presented in the previous section has been performed using the data obtained during 7 days of continuous monitoring of an external post-tensioning tendon belonging to a highway road bridge in Spain. The bridge monitored is a precast segmental externally post-tensioned bridge consisting of simply supported spans. The tendons monitored were grouted tendons made of 31 high-strength steel post-tensioning strands, each one made of 7 twisted wires of 6 mm of diameter. These strands were embedded inside a HDPE duct of 140 mm of diameter. Once tensioned, the duct was filled with grout to provide corrosion protection. This grout provides a monolithic effect to the tendon's section, which confers it a non-negligible bending stiffness. The accelerometers used were PCB-393B12 and were mounted using a clamp system attached to the tendon duct with bolts. Figure 10 depicts the bridge object of the study. The cable section being monitored is highlighted in red. Figure 11 shows the accelerometer mounted on the tendon.

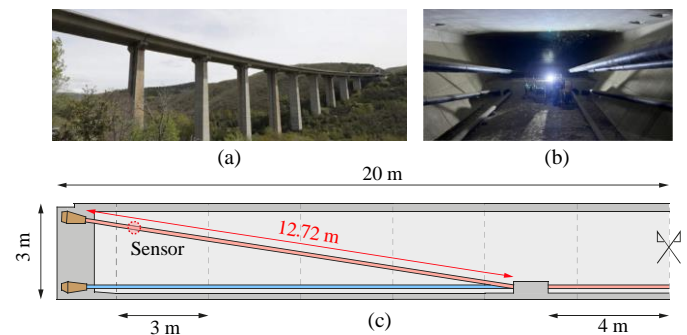


Figure 10: Description of the tendon being monitored

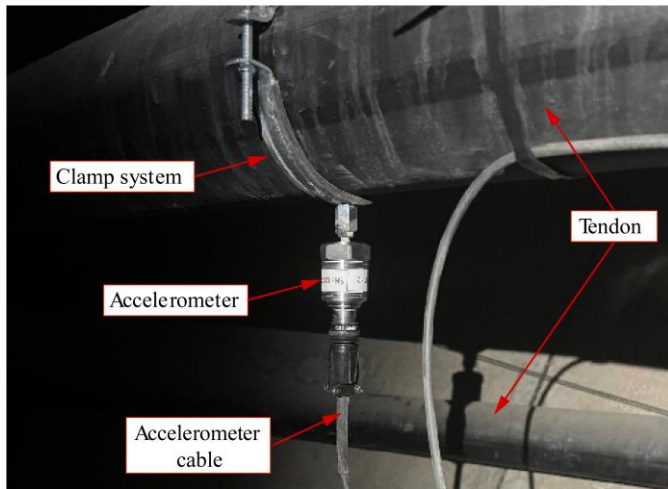


Figure 11: Accelerometer mounted on a tendon.

3.1 Analysis of a single data block

A single 10-minute data block has been analysed here to demonstrate the usefulness of the presented autonomous peak-picking methodology. The signal was acquired with a sampling frequency of 1651 Hz. The time-history and the corresponding PSD of this data block is shown in Figure 12.

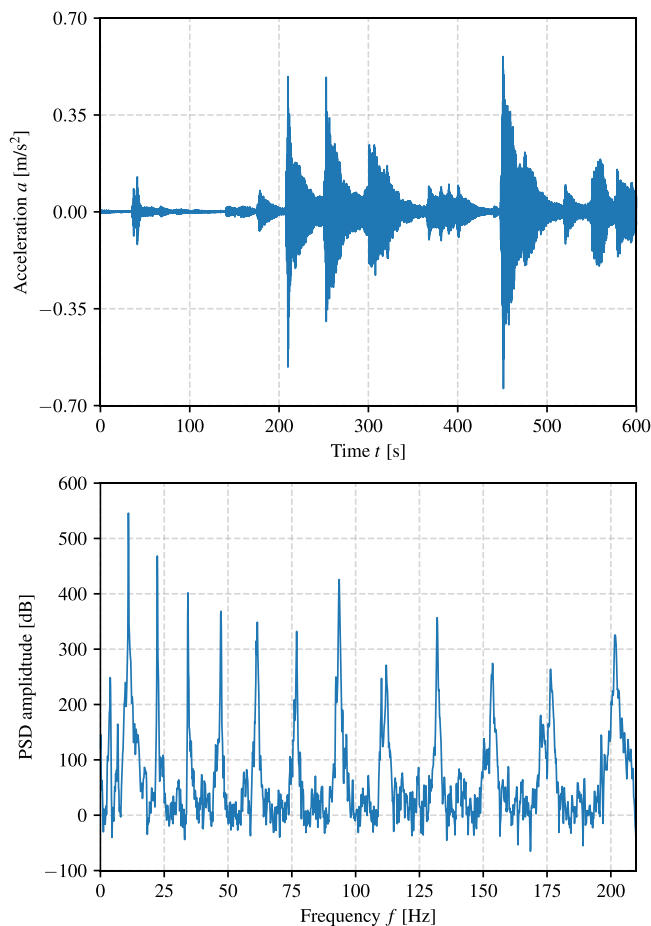


Figure 12: Analysis of a 10-minute data block.

The peaks detected present the noticeable effect of the bending stiffness, this effect can be seen in Figure 13, where the first 4 natural frequencies show a linear trend while starting

from the fifth natural frequency the data starts to show a non-linear trend.

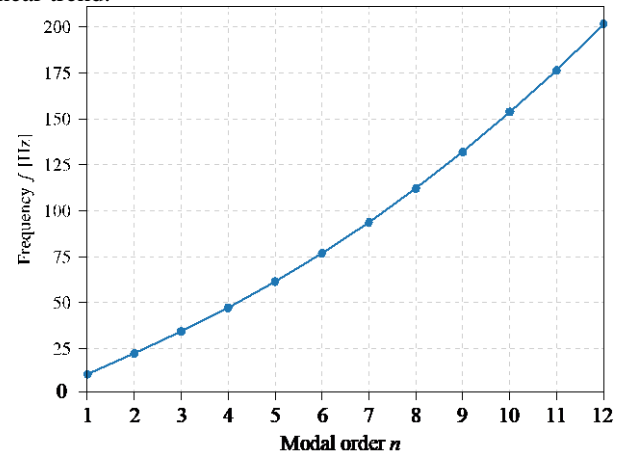


Figure 13: Modal order vs Frequency of a single data block.

3.2 Analysis of a one-day long data set

The variation of the different natural frequencies on the cable due to the temperature effect through one day has been firstly analysed. For that, the absolute frequency variation with respect to the initial frequencies being identified (those of the first 10-minutes record at 00:00) has been computed. Figure 14 shows this variation. It can be appreciated that the 4th modal order presents a slightly different behaviour this is due to its associated doublet. From this analysis, it can be also recognized how this variation is higher for higher modal orders.

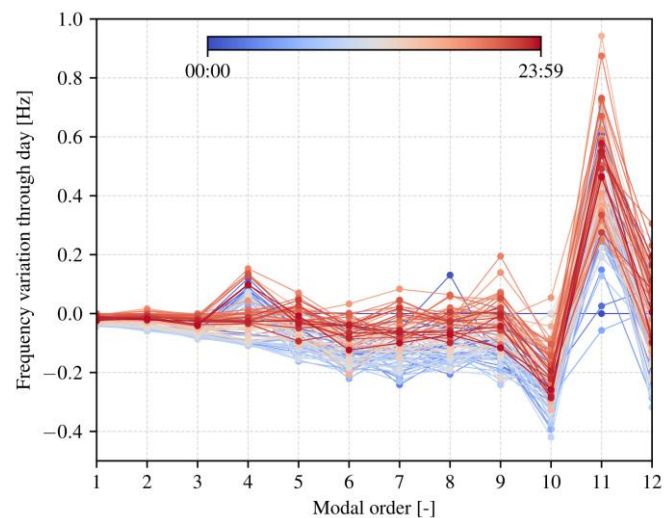


Figure 14: Temperature variation relative to the ones recorded at 00:00.

3.3 Analysis of a one-week long data set

Figure 15 shows the first 12 natural frequencies identified using the presented methodology. From the analysed data set, it can be confirmed the influence of temperature variation over frequency. While this variation is small, knowing its magnitude is fundamental to distinguish between environmental or damage variations. These results confirm the validity of the methodology applied and its use within a continuous monitoring loop.

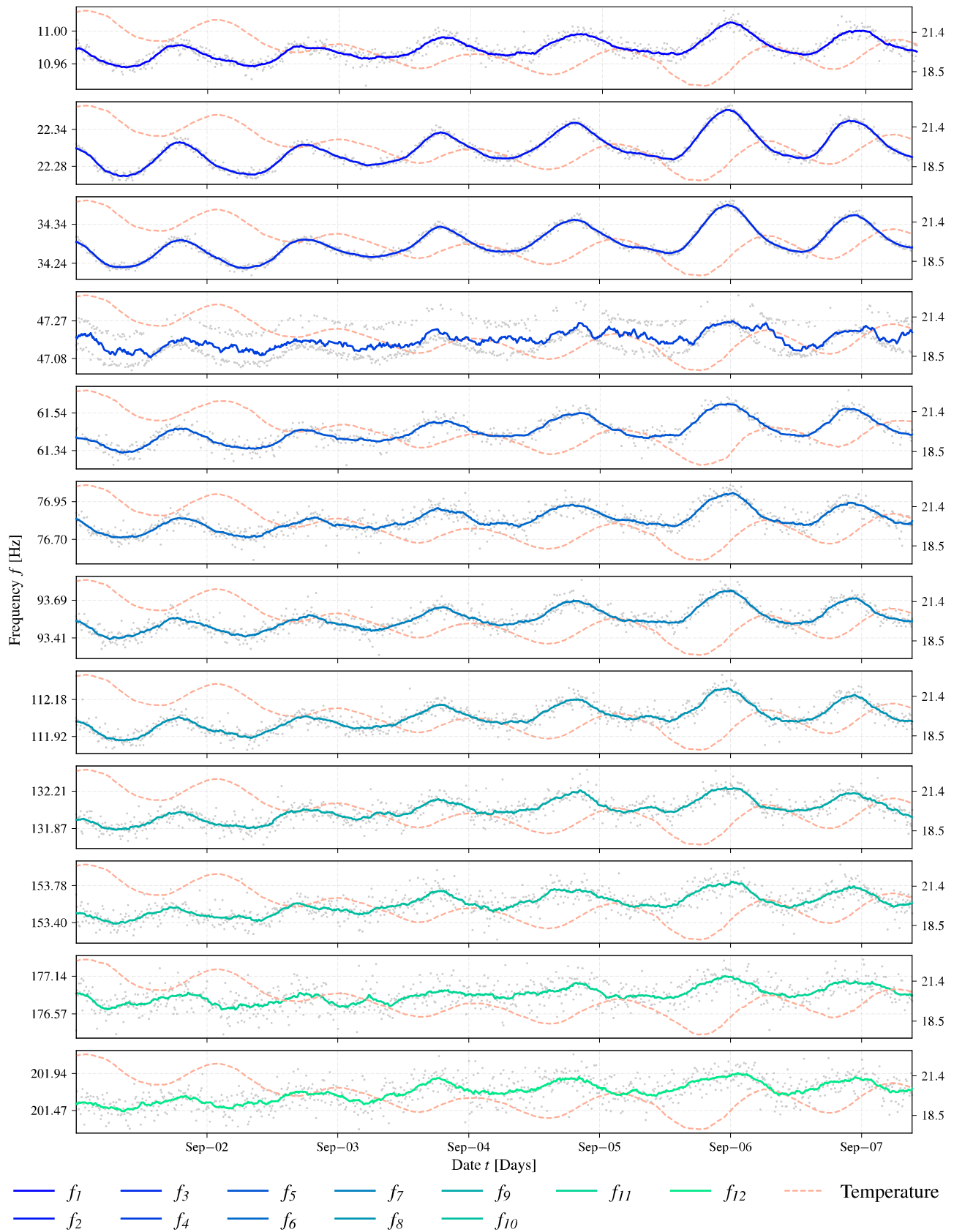


Figure 15: Complete frequency distribution along the week-long continuous monitoring.

4 CONCLUSIONS

An autonomous pick-picking procedure based on two PSDs (low and high resolution PSDs) combined with the use of a LMS procedure has been presented. The methodology has been conceived for its inclusion in continuous monitoring systems and to perform in-line tension force estimation since computation costs have been considered within the proposed methodology. From the results obtained from the one-week long monitoring data, it has been shown the performance of the proposed methodology.

Finally, some future works may include the autonomous identification of missing frequencies by the method, which can difficult cable tension estimation as this calculation depends on the natural frequencies and their corresponding modal orders correctly identified. Aside from this, the inclusion of the optimized asymmetric least squares (O-ALS) [4] baseline correction method which does not need hyperparameters fine tuning could be included.

ACKNOWLEDGMENTS

Supported by Research project PID2021-127627OB-I00 funded by MCIN AEI/10.13039/501100011033/FEDER, EU and Fundación Agustín de Betancourt.

REFERENCES

- [1] Scholkmann, F., Boss, J., & Wolf, M. (2012). An Efficient Algorithm for Automatic Peak Detection in Noisy Periodic and Quasi-Periodic Signals. *Algorithms*, 5(4), 588–603. <https://doi.org/10.3390/a5040588>
- [2] Jin, S.-S., Jeong, S., Sim, S.-H., Seo, D.-W., & Park, Y.-S. (2021). Fully automated peak-picking method for an autonomous stay-cable monitoring system in cable-stayed bridges. *Automation in Construction*, 126, 103628. <https://doi.org/10.1016/j.autcon.2021.103628>
- [3] Eilers, P. H. C. (2003). A Perfect Smoother. *Analytical Chemistry*, 75(14), 3631–3636. <https://doi.org/10.1021/ac034173t>
- [4] Dong, Z., & Xu, J. (2024). Baseline estimation using optimized asymmetric least squares (O-ALS). *Measurement*, 233, 114731. <https://doi.org/10.1016/j.measurement.2024.114731>
- [5] Cho, S., Lynch, J. P., Lee, J.-J., & Yun, C.-B. (2010). Development of an Automated Wireless Tension Force Estimation System for Cable-stayed Bridges. *Journal of Intelligent Material Systems and Structures*, 21(3), 361–376. <https://doi.org/10.1177/1045389X09350719>
- [6] Sim, S.-H., Li, J., Jo, H., Park, J.-W., Cho, S., Spencer Jr, B. F., & Jung, H.-J. (2014). A wireless smart sensor network for automated monitoring of cable tension. *Smart Materials and Structures*, 23(2), 025006. <https://doi.org/10.1088/0964-1726/23/2/025006>
- [7] Kim, H., & Sim, S. (2019). Automated peak picking using region-based convolutional neural network for operational modal analysis. *Structural Control and Health Monitoring*, 26(11). <https://doi.org/10.1002/stc.2436>
- [8] Jeong, S., Kim, H., Lee, J., & Sim, S.-H. (2021). Automated wireless monitoring system for cable tension forces using deep learning. *Structural Health Monitoring*, 20(4), 1805–1821. <https://doi.org/10.1177/1475921720935837>
- [9] Chen, Z.-W., Ruan, X.-Z., Liu, K.-M., Yan, W.-J., Liu, J.-T., & Ye, D.-C. (2022). Fully automated natural frequency identification based on deep-learning-enhanced computer vision and power spectral density transmissibility. *Advances in Structural Engineering*, 25(13), 2722–2737. <https://doi.org/10.1177/13694332221107572>
- [10] Zhang, M., He, H., Li, G., & Wang, H. (2021). Fully Automated and Robust Cable Tension Estimation of Wireless Sensor Networks System. *Sensors*, 21(21), 7229. <https://doi.org/10.3390/s21217229>
- [11] Wu, W.-H., Chen, C.-C., Lin, S.-L., & Lai, G. (2023). A Real-Time Monitoring System for Cable Tension with Vibration Signals Based on an Automated Algorithm to Sieve Out Reliable Modal Frequencies. *Structural Control and Health Monitoring*, 2023, 1–25. <https://doi.org/10.1155/2023/9343343>
- [12] Yuan, Y., Au, F. T. K., Yang, D., & Zhang, J. (2024). Active learning guided automated cable force monitoring based on modified S-transform. *Measurement*, 224, 113880. <https://doi.org/10.1016/j.measurement.2023.113880>